Ren *et al. Geoenvironmental Disasters* (2024) 11:1
https://doi.org/10.1186/s40677-023-00258-1

Geoenvironmental Disasters

RESEARCH

Open Access

Anchorage mechanism of bamboo-steel composite rockbolts subjected to the coupled effect of tensile and shear stress

Feifan Ren[1], Qiangqiang Huang[1], Guan Wang[2*] and Zhuang Li[1]

Abstract

Background Earthen heritage sites have high cultural and scientific value. However, most of earthen heritage sites have been severely damaged and are in urgent need of restoration. To address this issue, a novel rockbolt, bamboo-steel composite rockbolt (BSCR), was proposed and widely employed in earthen site protection. However, the research on the anchorage mechanism of BSCR lags behind engineering practice, particularly with regard to its behavior under the coupled effect of tensile and shear stress.

Case Presentation In this study, based on centrifugal test results, a numerical model was established and validated and a comparative analysis of the anchorage mechanism between conventional rockbolt (CR) and BSCR was also conducted. Various parameters, including rockbolt diameter, bending stiffness, inclination angle, and length, were systematically investigated to elucidate their influence on protective efficacy.

Conclusion BSCR has a larger diameter and bending stiffness, and is superior to CR in protecting earthen heritage sites. In addition, reducing the rockbolt inclination angle and increasing the number of rockbolt layers can reduce slope deformation caused by the coupling effect of tensile and shear stress. Increasing the length of BSCR can enhance the stability of the anchored slopes; however, due to the influence of the effective anchorage length of the rockbolt, excessively extending the rockbolt length is inefficient. These research results provide valuable insights into the application of BSCR in earthen site protection and can provide a reference for further research on its anchorage mechanism under complex stress conditions.

Keywords Earthen heritage site protection, Bamboo-steel composite rockbolt, Coupled effect of tensile and shear stress, Anchorage mechanism, Numerical study

Introduction

Ancient sites are of increasing importance to many countries as they represent a crucial part of human civilization (Hemeda 2018). These sites possess significant scientific, historical, and artistic value, and are non-renewable resources. Among these sites, earthen heritage sites are particularly vulnerable to environmental erosion and susceptible to damage from geological disasters (Tempa and Yuden 2023). Therefore, it is crucial to focus on the protection of earthen heritage to ensure its preservation for future generations (Li et al. 2020; Pei et al. 2020; Romanazzi et al. 2019). In the case of the Jiaohe Ruins in China, as depicted in Fig. 1, its predominant formation can be attributed to river erosion, resulting in the creation of a 30-m-high elongated platform. This site is classified as a natural raw soil architectural heritage site, in which, most buildings in Jiaohe Ruins were excavated

*Correspondence:
Guan Wang
wangguan@usst.edu.cn
[1] Key Laboratory of Geotechnical and Underground Engineering of Ministry of Education, Department of Geotechnical Engineering, Tongji University, Shanghai 200092, China
[2] School of Environment and Architecture, University of Shanghai for Science and Technology, Shanghai 200093, China

Fig. 1 **a** Jiaohe ruins in China, **b** Photo of BSCR

from the earth, partially constructed with it, or a combination of man-made materials, including rammed earth, mud bricks, and cob (Shao et al. 2013). Despite the high soil strength caused by the arid and hot climate and mineral cementation, these buildings have undergone severe weathering and rupture over thousands of years, mainly due to rainfall and wind erosion. Many earthen heritage sites have suffered serious structural damage and require restoration (Wang et al. 2022). Despite many efforts to promote the protection of earthen heritage sites over the past few decades, it cannot be denied that the technology for protecting these sites is not yet mature (Correia 2016; Richards et al. 2018, 2020).

The restoration of earthen heritage sites requires strict adherence to principles aimed at retaining their appearance and minimizing any structural damage. To achieve these goals, anchorage technology has become a popular solution widely employed by cultural relic protection departments. Rockbolts are a critical component of this approach as they require minimal soil excavation, and upon installation, they can be buried in the soil while the surface is covered with on-site soil. However, conventional rockbolts (CRs) are not suitable for earthen heritage site protection (Wang et al. 2022), as it is typically composed of steel bar/strands, which implies high costs, especially when used in large quantities. Furthermore, its structural strength would continuously decrease over time, making it challenging to satisfy prolonged performance criteria. Additionally, the soil at earthen heritage sites is loose and soft, and due to the relatively small diameter of CR, it struggles to provide sufficient anchoring force. To solve the shortcomings of CRs, bamboo-steel composite rockbolts (BSCR) were proposed (Ren et al. 2009), and the appearance is shown

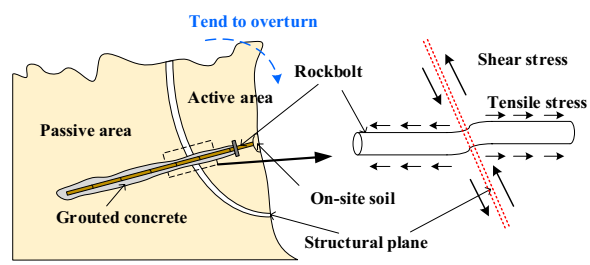

Fig. 2 Stress distribution of rockbolt in earth heritage site

in Fig. 1b. The primary material used in BSCR is bamboo, a natural substance that offers advantages in terms of cost-effectiveness and robust corrosion resistance. Additionally, the relatively large diameter of BSCR contributes to its substantial bending stiffness, high pull-out resistance, similar deformability with soil and significant anchoring force. These attributes collectively play a crucial role in preserving the stability of earth heritage sites. The BSCRs have been successfully applied to the Ruins of Jiaohe, Gaochang and Juyan in China. Despite their successful application, research on the anchorage mechanism of BSCR is significantly lagging behind engineering practice (Ren et al. 2012). Furthermore, anchors within the soil consistently experience complex stress conditions, characterized by combined tensile and shear stresses, as depicted in Fig. 2. Therefore, it is imperative to investigate the anchorage mechanism of BSCRs, especially under the coupled effect of tensile and shear stress (Takase 2019).

The present study aims to investigate the anchorage mechanism of BSCR under the coupled effect of tensile and shear stress, utilizing the finite element analysis method. The methodology involves validating a finite

element model through centrifuge model tests, followed by a parametric study to analyse the influence of various design parameters, including the inclination angle of rockbolt, the number of anchorage layers, and the length of the rockbolt. The findings of this investigation have implications for optimizing the engineering design of BSCR and improving its effectiveness in the preservation of earthen heritage sites. Consequently, this research contributes to the practical application of BSCR technology in heritage site protection projects.

Materials and methods

BSCR structure

BSCR is a composite reinforcement composed of bamboo, composite fillers, and steel strands. The manufacturing process of BSCR involves several steps. Initially, a bamboo with a diameter of approximately 100 mm is chosen and then split into two sections along the radial direction. These sections are subsequently filled with a composite filler, which is a mixture of fly ash, epoxy resin, asbestos, alcohol and curing agent. Next, the two halves of the bamboo are brought together with a steel strand positioned at the center, and bundled with steel straps at intervals of 0.5 m. Finally, the bundled bamboo is wrapped with glass cloth and coated with epoxy resin to enhance corrosion resistance. A diagram and photograph of the cross-section of BSCR are displayed in Fig. 3. The mechanical properties of BSCR are derived from the high strength and toughness of bamboo, the reinforcing function of the inner steel strand, and the composite filler, which serves to bond the bamboo and steel strand together and transfer loads from the bamboo to the steel strand (Ren et al. 2010; Zhang et al. 2015). Through on-site tests at the Jiaohe Ruins, Zhang et al. (2015) found that the ultimate pull-out resistance of BSCR with a length of 5 m and a diameter of 95 mm can reach over 200 kN, showing the substantial potential of BSCR for reinforcing earthen heritage sites.

The specific installation steps for BSCR are shown in Fig. 4 (a)–(i): (a) Use a drilling rig to bore holes at specified locations within the soil site that require reinforcement, ensuring the holes are straight to maximize the reinforcing effect of the BSCR; (b) After completing the drilling, thoroughly clean the soil inside the holes; (c) Attach two ropes to the front and rear parts of the BSCR and carefully hoist it onto the work platform. The purpose of these two ropes is to facilitate the control of the BSCR and prevent any damage to it during the lifting process. (d) Insert the BSCR into the drilled holes. (e) Perform grouting inside the holes. (f) Grouting completed; (g) Install the anchor plates. (h) Seal the holes using on-site soil and make necessary adjustments; (i) Installation completed.

Centrifuge model tests

To investigate the anchorage mechanism of rockbolts under the coupled effect of tensile and shear stress, a series of centrifugal model tests on bolted slopes were performed at 18 gravities using a centrifuge facility at Tongji University, Shanghai, China. The details of this centrifuge facility were described in detail by Huang et al. (Huang et al. 2020). To ensure the results of centrifuge model tests are comparable to those of a prototype, it is crucial to correctly scale down the parameters of the centrifuge model experiment based on the similitude laws and select appropriate materials (Ren et al. 2020a, b). The details of the scaling laws adopted for the centrifuge model tests are listed in Table 1. The model slopes in the tests were 500 mm high, equivalent to a 9 m high slope in prototype. Over the span of the past decade, extensive research endeavors have been dedicated to investigating the fundamental physical properties of soils within the confines of the Jiaohe ruins, as detailed by Shao et al. (2013). Building upon the findings of these previous studies and the scaling laws listed in Table 1, some key parameters, namely uniaxial compressive strength,

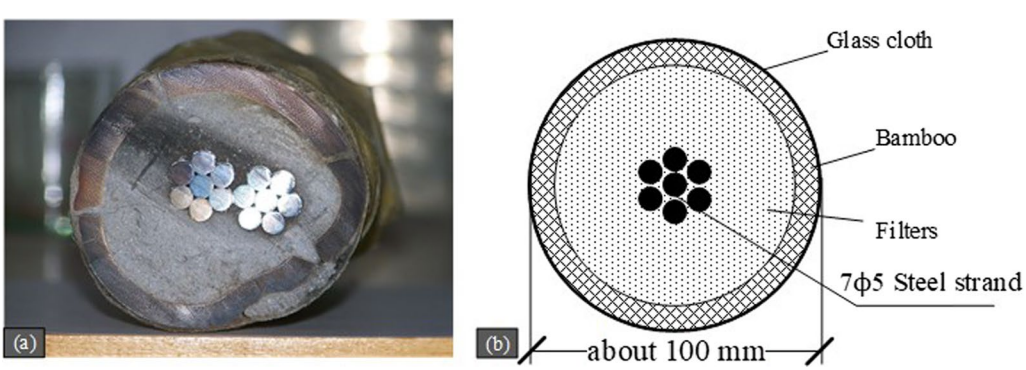

Fig. 3 **a** Photo of the BSCR cross section, **b** Schematic drawing of the BSCR cross section

Fig. 4 Installation procedure of the BSCR

Table 1 Main scaling laws adopted for centrifuge model tests

Parameters	Prototype	Model
Soil of slope		
Density (ρ_s)	1	1
Young's modulus (E_s)	1	1
Cohesion (c)	1	1
Friction angle (φ)	1	1
Rockbolts		
Bending stiffness (B)	1	1/N
Tensile strength (T)	1	1/N
Diameter (D)	1	1/N

N = model ratio

Table 2 Properties of model soil used in the tests

Properties	Unit	Value
Uniaxial compressive strength: q_u	kPa	585
Secant modulus: E_{50}	MPa	42
Density: ρ_s	g/cm^3	2.03
Cohesion: c	kPa	148
Friction angle: φ	°	30

secant modulus, density, cohesion, friction angle, have been confirmed for this study. The slope soil was modeled using a mixture of silica sand, clay, cement, and water. Through a comparative analysis of uniaxial compression test results on model soil with varying cement ratios, it was observed that an incremental rise in cement content led to a corresponding enhancement in the strength of the model soil. Notably, a model soil sample with a 9% cement mass ratio exhibited a density of 2.03 g/cm3 and an elastic modulus of 42 MPa. This contrasted with the density of approximately 2 g/cm3 and an elastic modulus of roughly 40 MPa found in the prototype soil of the Jiaohe ruins. According to the similarity law of centrifugal model, the physical and mechanical

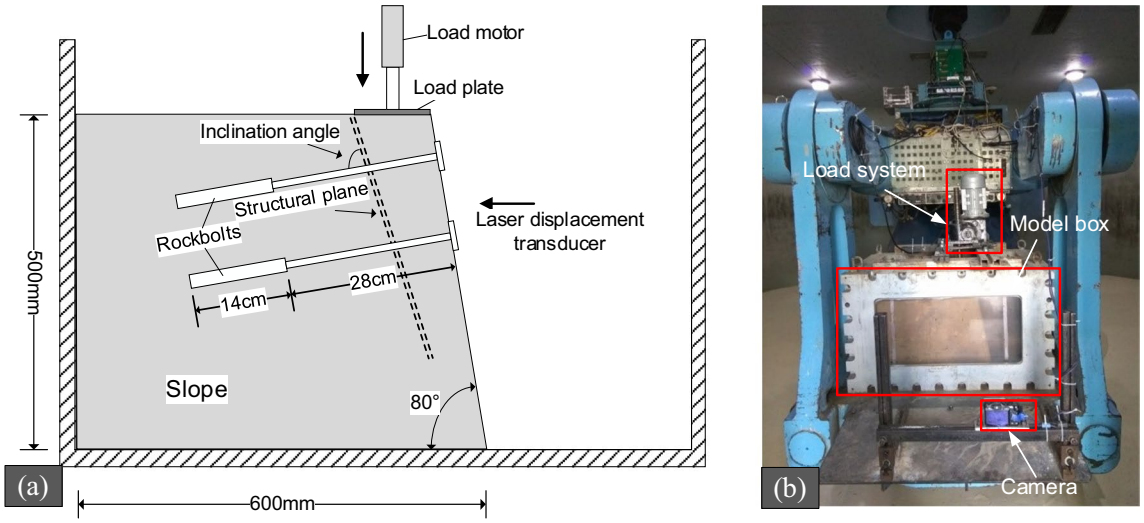

Fig. 5 Centrifuge model test **a** Layout of the slope with the locations of measuring sensors **b** Centrifuge model

properties of the model soil are very similar to the prototype soil. Therefore, the mass ratio of each component in the model soil is determined as silica sand: clay: cement: water = 8:2:0.9:2.18, and the curing period is 7 days. The detailed mechanical characteristics of the model soil are presented in Table 2. During the casting process of slope models, a fissure (72° from the bottom, 370 mm in length), consisting two-layer poly tetra fluoro ethylene (PTFE) films coated with lubricating oil, was pre-embedded at a distance of 130 mm from the top of the slope surface. Two types of rockbolts, made of organic glass (polymethyl methacrylate) and steel wire, were employed to simulate BSCR and CR respectively. It should be noted that the two kinds of rockbolts have the same axial stiffness but different bending stiffness, that is to say, BSCR can bear much more lateral shear stress than CR. The loading system was composed of a load plate (dimensions: 130 mm × 130 mm × 25 mm) and a load motor with a constant loading rate of 15 mm/min.

The top settlement and lateral deformation of the slope face were measured by two laser displacement transducers. The particle image velocity (PIV) technique was used to determine the global deformation of the slope by comparing high-definition digital camera photos captured before and after loading (Li and Jing 2008). In addition, the strains of rockbolts were measured using strain gauges. The layout of the slope with locations of measurement sensors and the centrifuge model are shown in Fig. 5. Five tests were carried out to investigate the anchorage mechanism of rockbolts with different parameters as listed in Table 3. A detailed description of the centrifuge tests and the analysis of the results can be found in Refs (Ren et al. 2018).

Table 3 Summary of model configurations

Test name	Rockbolts material	Number of layers
Case NR	–	–
Case 1	Steel wires	1
Case 2	Organic glass	1
Case 3	Steel wires	2
Case 4	Organic glass	2

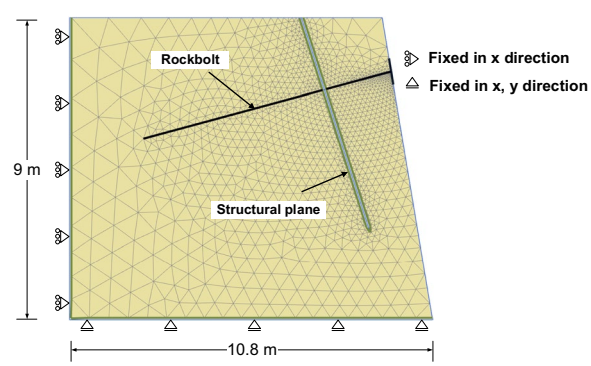

Fig. 6 FEM mesh used in simulation (Prototype)

Finite element simulation

The finite element program PLAXIS was employed to simulate the aforementioned centrifuge model test. In order to investigate the anchorage mechanism of the rockbolts subjected to the coupled effect of lateral tensile and shear stress in practice engineering, the scale of the numerical model was consistent with the prototype

Table 4 Material parameters of slope

Materials	Elastic modulus *E* (Mpa)	Poisson's ratio v	Cohesion *c* (kPa)	Internal friction angle *φ* (°)
Slope soil	40	0.25	148	30
Structural plane	0.35	0.35	2	10

Table 5 Material parameters of BSCR and CR

Materials	Axial stiffness *EA* (kN)	Bending stiffness *EI* (kN·m^2)	Diameter *D* (cm)
BSCR	3.18×10^4	4.96	10
CR	3.18×10^4	0.042	2

of the centrifuge test. That is, a 9 m high and 10.8 m long slope was numerically built, with the bottom fixed and the sides set to be horizontally fixed, as shown in Fig. 6. BSCR was simulated by plate elements, and the CR was simulated by spring elements, and the structural plane was simulated by interface elements. The plate elements can bear tensile stress and shear stress, while the spring elements can only bear tensile stress. In this investigation, it is assumed that both the plate elements and spring elements are elastic. The Mohr–Coulomb failure criterion was used for modelling the behaviour of soil and structural plane in this study, a technique widely utilized by scholars in finite element analysis (Ardakani et al. 2014; Argani and Gajo 2021; Jia et al. 2010). Material properties of the slopes and rockbolts used in the numerical model were determined through laboratory testing, and are summarized in Table 4 and Table 5.

Verification of the finite element model

To ensure the validity of the finite element model and effectively simulate the mechanical behavior of BSCR, it is necessary to verify its accuracy. In this study, combined with the results of the centrifugal model tests (Ren et al. 2018), the verification of the finite element model was conducted by means of a comparative analysis involving the slope bearing capacity, deformation and axial stresses along the rockbolt.

Bearing capacity

The load–displacement relationship plays a vital role in evaluating the load-bearing capacity of bolted slopes and the effectiveness of rockbolts, making it a significant parameter in engineering practices. Through a comparison between the load–displacement curves obtained from five centrifuge test results and the corresponding calculated results presented in Fig. 7, the numerical results are good agreement with the centrifuge test results. In addition, the load–displacement curves of the bolted slopes (Case 1–Case 4) in centrifuge tests, as shown in Fig. 7b-e, can be characterized by three consecutive stages: elastic, plastic and failure. Initially, during the elastic stage at the initial loading phase, there is a rapid increase in the vertical load, leading the bolted slopes to reach the plastic point with a minimal vertical

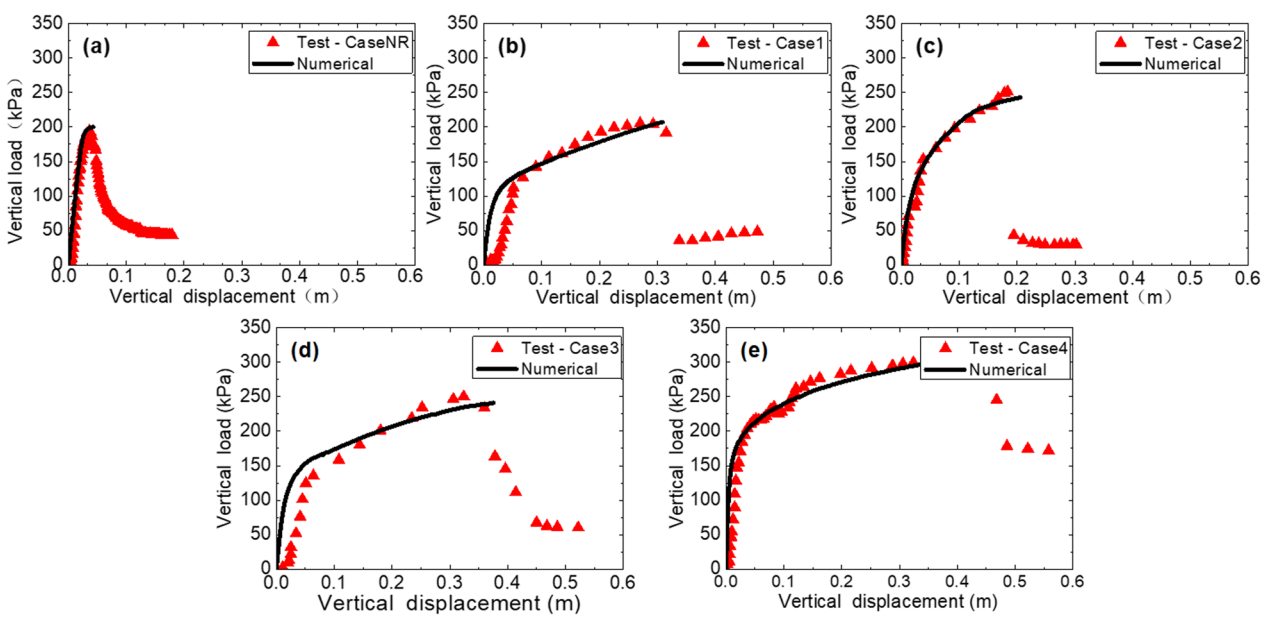

Fig. 7 Comparison of centrifuge test results with calculated results of load bearing capacity

displacement of approximately 0.05 m. Subsequently, as the plastic stage commences, the growth rate of the vertical load diminishes significantly with the progressive increase in vertical displacement, indicating the onset of yielding in the rockbolts. Towards the end of the plastic stage, there is a sharp decline in loading corresponding to the increase in vertical displacement, marking the transition of the slopes into the failure stage, characterized by rockbolt yield failure. In contrast, the load–displacement curve of the slope without any reinforcement (Case NR), as shown in Fig. 6a, can be roughly divided into two stages of elastic and damage. Following the elastic stage, the fractured soil entered directly into the damage stage, aligning with the inherent characteristics of the soil. Furthermore, upon comparing Fig. 7b and c, it becomes evident that BSCR exhibits a superior load-bearing capacity in comparison to CR. This distinction arises from the fact that CR, due to its smaller diameter, is more prone to cutting into the soil (Spang and Egger 1990). On the other hand, the larger diameter of BSCR has a higher bending stiffness and can effectively mitigate this problem.

Deformation and failure mode

As mentioned in the section of Centrifuge model tests, the displacement vector magnitude and shear strain of slopes could be obtained by the PIV technology. However, due to the limitation of the observation window size of the model box, only the area within the red dotted box shown in Fig. 8a was taken for analysis. In addition, as the anchorage mechanism of BSCR is the main focus of this research, the centrifuge test of Case 2, which replicated BSCR in prototype, was chosen for numerical comparison. Figure 8b and c show the displacement vector magnitude and shear strain of the centrifugal slope model at failure in Case 2 respectively. It can be seen that the slope deformation mainly occurs in the sliding soil body on the right side of the structural plane. The shear strain mainly accumulates in the lower part of the sliding soil and at the intersection of the sliding surface and the rockbolt. This phenomenon could potentially be attributed to stress concentration resulting in localized loosening of the soil medium. The displacement and shear strain nephograms of the numerical results are shown in Fig. 8d and

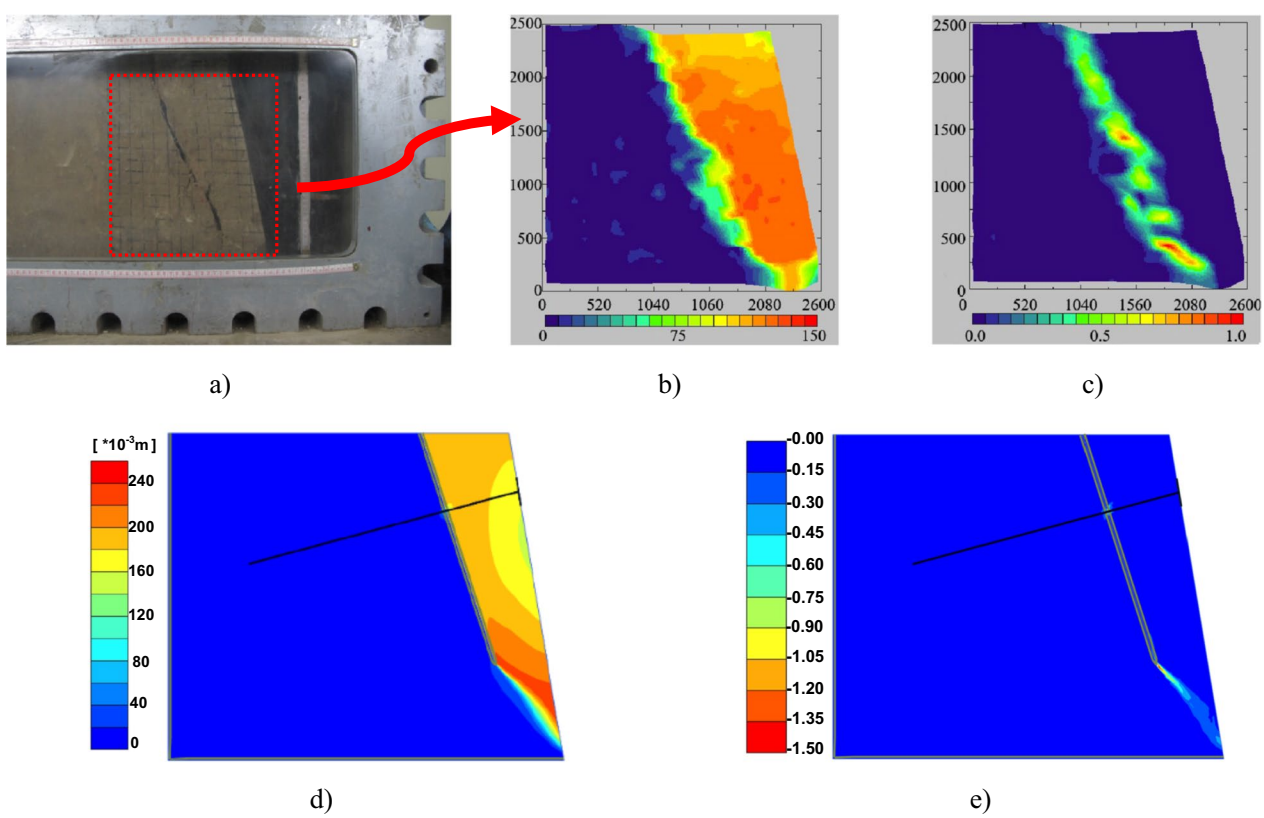

Fig. 8 Displacement vector magnitude and shear strain of the slope at failure (Case 2) **a** Centrifuge model photo **b** Displacement vector magnitude in model test **c** Shear strain in model test **d** Displacement vector magnitude in numerical simulation **e** Shear strain in numerical simulation

e, which are similar to the experimental results in terms of tendency and magnitudes. In other words, the numerical simulation agrees well with the centrifuge test on the whole.

Axial stress of rockbolt

Figure 9 presents a comparison between the measured and calculated axial stress distribution along the rockbolt under a vertical load of 250 kPa, where positive values indicate tensile stress and negative values indicate compression stress. It can be observed that the calculated results are slightly lower than the measured results, but the overall distribution of axial stress is nearly identical. It should be noted that the axial strain of rockbolt, obtained from the strain gauge readings, may be influenced by various factors such as installation and calibration-strain relationship, as mentioned by Ren et al. (Ren et al. 2016). Therefore, the difference between the measured and the calculated axial stress of rockbolt in this study is still acceptable. This analysis further substantiates the higher precision of the finite element analysis employed in this study, thereby providing a solid foundation for conducting further investigations into the anchorage mechanism of BSCR.

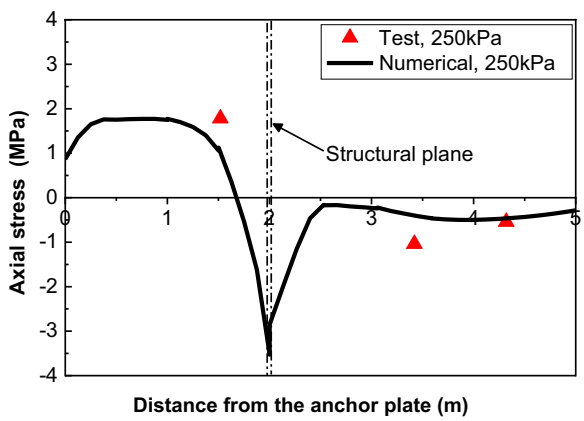

Fig. 9 Distribution of axial stress along rockbolt (Case 2)

Parametric analysis

Although the results of model tests are generally reliable, the testing process can be both time-consuming and costly, making it arduous to perform a considerable number of tests. With the development of computer technology, the alternative method of finite element analysis has been widely used by many scholars and achieved good results. To further investigate the influence of design parameters, a parametric study was performed using the finite element analysis in this study, in which the centrifugal test of Case-2 was chosen as the benchmark group. This approach allowed for a comprehensive exploration of the impact of various design parameters, while leveraging the benefits of computational analysis.

Effect of the rockbolt inclination angle

The inclination angle α, which represents the angle between rockbolt and structural plane (as shown in Fig. 5a), is a significant factor influencing the mechanical

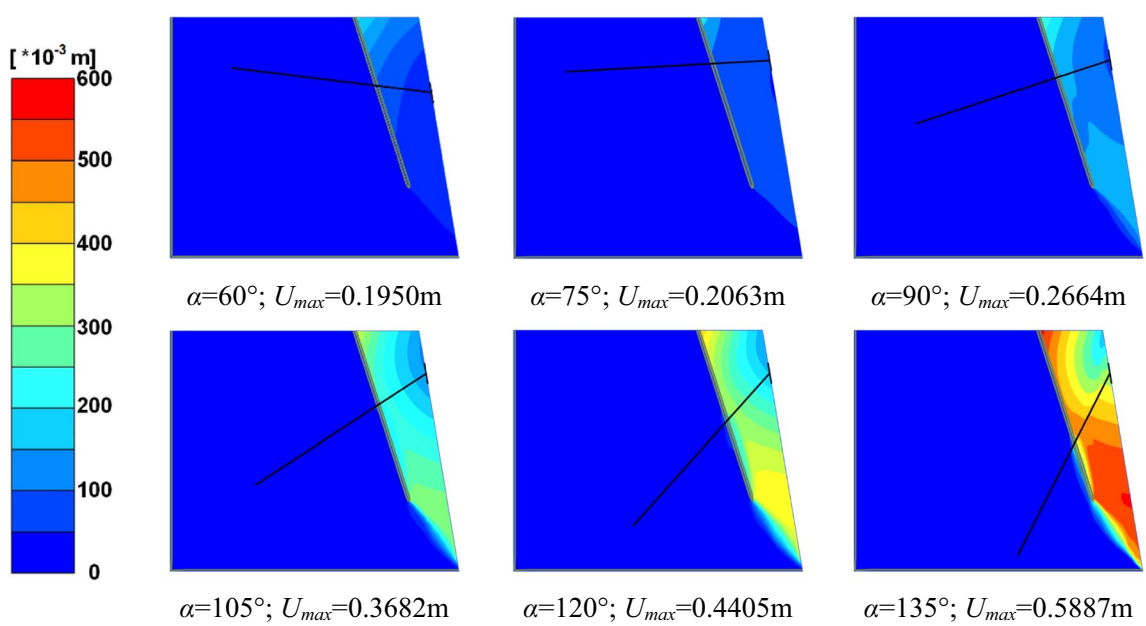

Fig. 10 The slope deformation for different rockbolt inclination angles

characteristics of rockbolts. This has been approved by numerous researchers (Chen 2014; Cui et al. 2020; Li et al. 2016). In this study, the impact of different rockbolt inclination angles on slope deformation under a load of 250 kPa was investigated, and the results are presented in Fig. 10. It can be observed that the slope deformation increases as the inclination angle becomes larger, with this trend becoming more pronounced for angles exceeding 90°. This phenomenon can be attributed to the fact that BSCR is more flexible and has a significantly greater capacity for tension than compression. Thus, BSCR performs better in terms of tensile strength when the rockbolt inclination angle is less than 90°. However, if the anchorage angle exceeds 90°, the rockbolt is subjected to higher compressive stress. These findings are supported by the distribution of axial stress along the rockbolt for different inclination angles, as illustrated in Fig. 11a. At an inclination angle of 60°, the axial stress values are predominantly positive, while at an anchoring angle of 135°, the values are entirely negative. This indicates that as the inclination angle of the rockbolt changes from 60° to 135°, it undergoes a gradual transition from tension to compression.

However, it is not suggested to reduce the inclination angle of the rockbolt too much, as this will make it difficult to fully utilize BSCR's lateral shear capacity. As shown in Fig. 11b, when the inclination angle is 90°, the maximum positive and negative values of the shear stress of the rockbolt are at a higher level, indicating that the shear capacity of BSCR is completely exerted in this state. Moreover, the two images depicting angles $\alpha = 60°$ and $\alpha = 75°$ in Fig. 10 demonstrate that reducing the inclination angle may not necessarily result in a significant reduction in slope deformation. Therefore, in practical engineering applications, it is advisable to choose an inclination angle slightly less than 90° to facilitate grouting operations while still maintaining a satisfactory level of performance.

Effect of the number of rockbolt layers

Figure 12 illustrates the effect of the number of BSCR layers on slope deformation under a vertical load of 250 kPa. The results demonstrate a decrease in slope deformation with an increase in the number of rockbolt layers. This observation aligns with expectations, as a greater

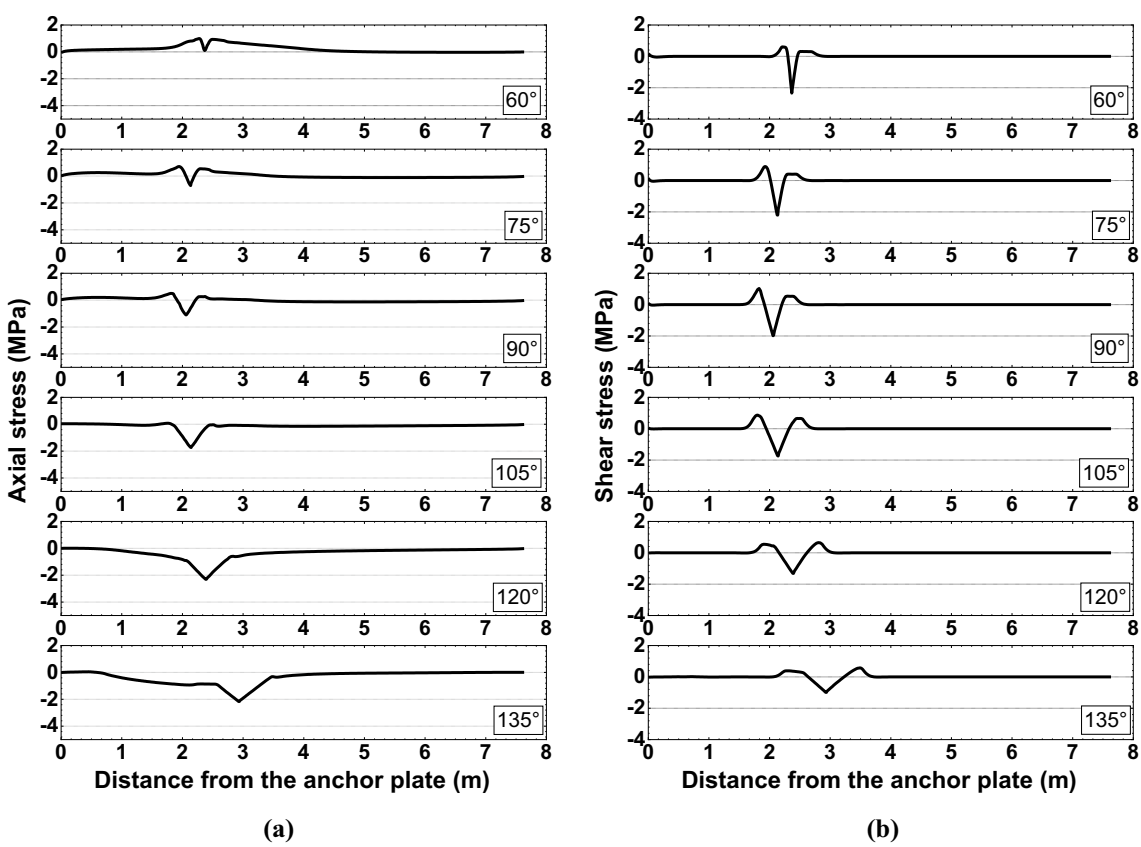

Fig. 11 **a** Axial stress and **b** shear stress distribution with different anchorage angle

number of rockbolt layers enhances the overall stiffness of the bolted slope, thereby increasing its resistance to deformation (Lin et al. 2020). Figure 13a and b depict the distribution of lateral displacement and settlement of the slopes with varying numbers of rockbolt layers. Notably, increasing the number of rockbolt layers from two to three results in only a 4.7% reduction in lateral displacement and a 13.8% reduction in settlement compared to increasing from one to two. Therefore, considering the principle of minimizing damage to earthen heritage sites, it is recommended to avoid excessive use of rockbolts while ensuring safety and effective deformation control.

Effect of the rockbolt length

Figure 14 shows the deformation of bolted slopes with varying rockbolt lengths. The slope deformation is the greatest with the smallest rockbolt length of 3 m, whereas there is no discernible difference between the slopes with rockbolt lengths of 7.6 m and 5 m. It is observed that reducing the rockbolt length from 5 to

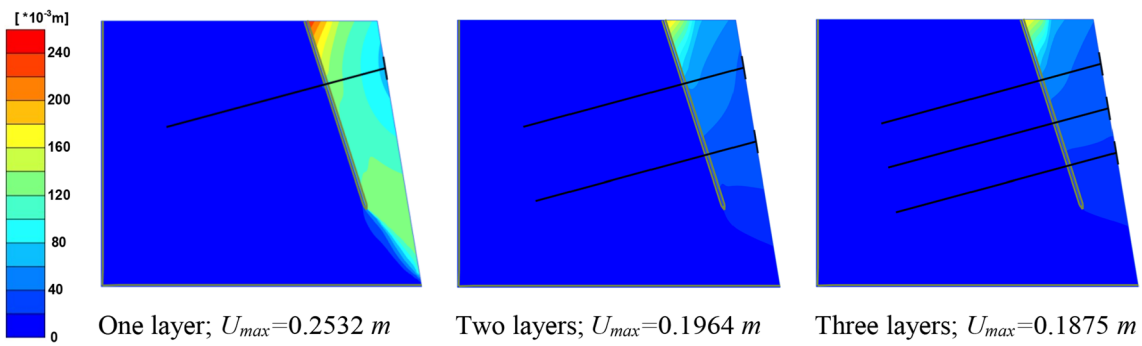

Fig. 12 Slope deformation with the number of rockbot layers

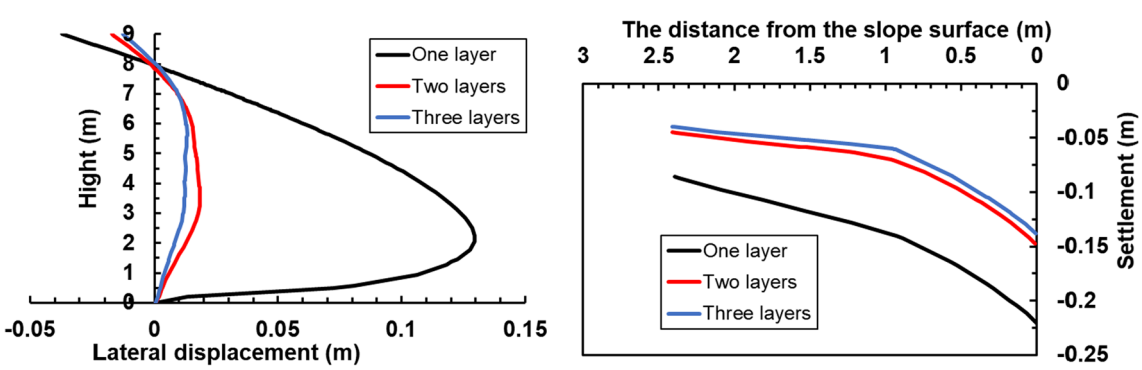

Fig. 13 The lateral displacement and settlement distribution with the number of rockbolt layers

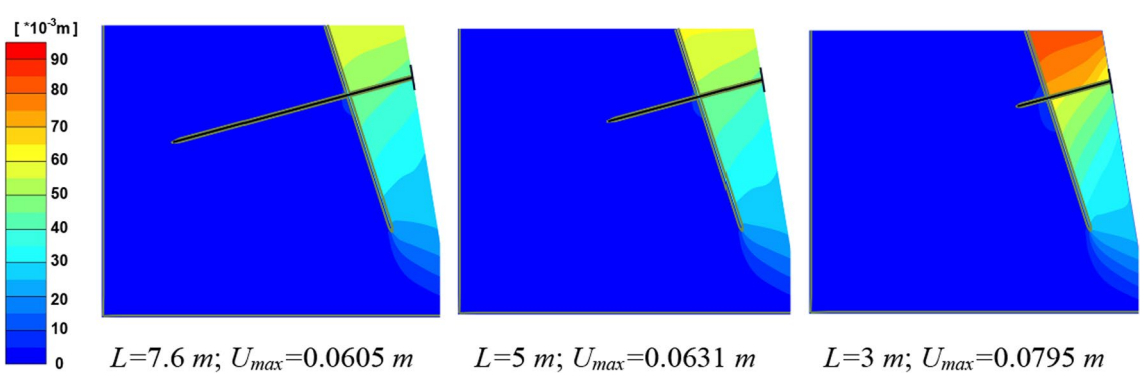

Fig. 14 Slope deformation of rockbolts with different length

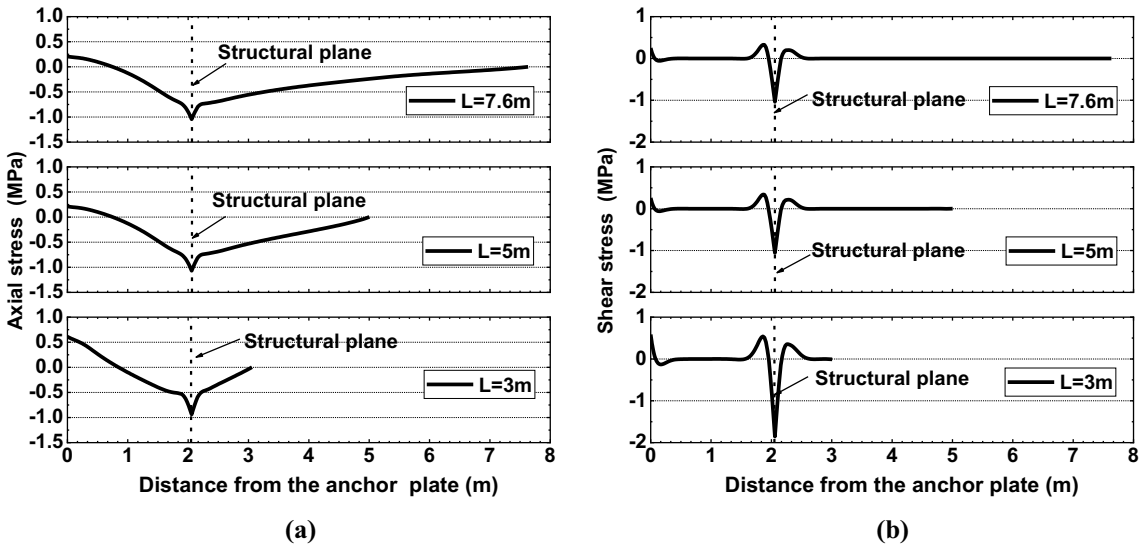

Fig. 15 **a** Axial stress and **b** shear stress distribution of rockbolts with different length

3 m leads to a ten-fold increase in slope deformation compared to a reduction from 7.6 m to 5 m. This indicates that increasing the rockbolt length can enhance slope stability, but excessively long rockbolts do not significantly improve it.

Figure 15a and b compares the axial stress and shear stress of rockbolts of various lengths. The axial stress distribution range of the shortest rockbolt is smaller than that of other rockbolts, indicating that it is too short to provide complete anchoring force. The axial stress distribution of the 7.6 m and 5 m rockbolts is nearly identical, meaning that the axial stress is very small beyond 5 m for the 7.6 m rockbolt. This finding suggests that the BSCR has an effective anchorage length of approximately 5 m, as supported by previous studies (Ren et al. 2018, 2020a, b). In addition, the length of the rockbolt has little effect on the distribution of shear stress, which is mainly concentrated near the structural plane.

In conclusion, the stability of bolted slopes could be improved by increasing the length of BSCR. However, due to the limitation of the effective anchorage length of the rockbolt, excessive lengthening of the rockbolt is wasteful. On the other hand, reducing the drilling depth of the rockbolt can be a way to preserve earthen heritage sites. However, considering the presence of cracks within the earthen heritage sites that continue to propagate internally, as indicated by the multi-layer crack structure in Fig. 1a, it is crucial to ensure a sufficient safety length of the rockbolt.

Conclusion

BSCRs have been widely employed to protect earthen heritage sites, but its anchorage mechanism is still unclear, especially under the coupled effect of tensile and shear stress. In this paper, combined with the results of centrifuge tests, the anchorage mechanism of BSCRs under the coupled effect of tensile and shear stress was investigated by the means of numerical simulation, and a parametric study was also carried out for providing further insights on the effect of the design parameters. The main conclusions are as follows:

1. Compared with CRs, BSCRs with larger bending stiffness could bear more load, and are more suitable for the protection of earthen heritage sites. The axial stress and shear stress experienced by the rockbolts primarily concentrate in or near the structural plane due to the coupled effect of tensile and shear stress.
2. The slope deformation increases with an increase of the inclination angle, and this trend becomes more pronounced when the angle exceeds 90°. In practical engineering applications, it is recommended to maintain the inclination angle slightly below 90° to maximize the lateral shear resistance of BSCR.
3. The slope deformation decreases as the number of BSCR layers increases. However, considering the principle of minimizing damage to earthen heritage sites, it is advisable not to utilize an excessive number of BSCR layers while ensuring safety and effective deformation control.

4. Increasing the length of BSCR can improve the stability of the slope. Nevertheless, due to the limitations imposed by the effective anchorage length, excessively lengthening the rockbolt is inefficient and wasteful.

In conclusion, this study provides valuable insights into the anchorage mechanism of BSCRs under the combined effect of tensile and shear stress. The findings highlight the superior load-bearing capacity of BSCRs compared to CRs, emphasize the significance of the inclination angle and number of BSCR layers in slope deformation control, and underscore the importance of optimizing the rockbolt length while considering the effective anchorage length. These conclusions contribute to a better understanding of BSCR behavior and provide practical guidance for the protection of earthen heritage sites.

Acknowledgements
This study was supported by Shanghai Pujiang Programme (23PJD101), the National Natural Science Foundation of China (41877224), the China Scholarship Council (202006265003) and the National Key Research and Development Plan of the Ministry of Science and Technology of the People's Republic of China (2019YFC1509900).

Author contributions
FR carried out numerical modelling and manuscript preparation. QH collected data and created figures. GW provided suggestions and advice to the study and checked the manuscript. ZL provided the results of centrifuge model tests. All Authors read and approved the final manuscript.

Availability of data and materials
Data and materials are available upon request.

Declarations

Competing interests
The authors declare no competing interests.

Received: 2 June 2023 Accepted: 7 November 2023
Published online: 02 January 2024

References

Ardakani A, Bayat M, Javanmard M (2014) Numerical modeling of soil nail walls considering Mohr Coulomb, hardening soil and hardening soil with small-strain stiffness effect models. Geomech Eng 6(4):391–401. https://doi.org/10.12989/gae.2014.6.4.391

Argani LP, Gajo A (2021) A new isotropic hyper-elasticity model for enhancing the rate of convergence of Mohr–Coulomb-like constitutive models and application to shallow foundations and trapdoors. Comput Geotech 132:103957. https://doi.org/10.1080/15583058.2019.1619881

Chen Y (2014) Experimental study and stress analysis of rock bolt anchorage performance. J Rock Mech Geotech 6(5):428–437. https://doi.org/10.1016/j.jrmge.2014.06.002

Correia M (2016) Conservation in earthen heritage: Assessment and significance of failure, criteria, conservation theory, and strategies. Cambridge Scholars Publishing, Cambridge

Cui G, Zhang C, Chen J et al (2020) Effect of bolt inclination angle on shear behavior of bolted joints under CNL and CNS conditions. J Cent South Univ 27(3):937–950. https://doi.org/10.1007/s11771-020-4342-x

Hemeda S (2018) Engineering failure analysis and design of support system for ancient Egyptian monuments in Valley of the Kings, Luxor, Egypt. Geoenviron Disasters. https://doi.org/10.1186/s40677-018-0100-x

Huang Y, Xu X, Liu J, Mao W (2020) Centrifuge modeling of seismic response and failure mode of a slope reinforced by a pile-anchor structure. Soil Dyn Earthq Eng 131:106037. https://doi.org/10.1016/j.soildyn.2020.106037

Jia S, Chen W, Yang J, Chen P (2010) An elastoplastic constitutive model based on modified Mohr–Coulomb criterion and its numerical implementation. Rock Soil Mech 31(7):2051–2058. https://doi.org/10.16285/j.rsm.2010.07.041

Li Y, Jing H (2008) Software development of a digital speckle correlation method and its application. J China Univ Min Techno 37(5):635–640. https://doi.org/10.3321/j.issn:1000-1964.2008.05.011

Li L, Hagan P, Saydam S et al (2016) Parametric study of rockbolt shear behaviour by double shear test. Rock Mech Rock Eng 49(12):4787–4797. https://doi.org/10.1007/s00603-016-1063-4

Li J, Zhang X, Xiao L et al (2020) Changes in soil microbial communities at Jinsha earthen site are associated with earthen site deterioration. BMC Microbiol 20:1–11. https://doi.org/10.1186/s12866-020-01836-1

Lin H, Zhu Y, Yang J (2020) Anchor stress and deformation of the bolted joint under shearing. Adv Civ Eng 2020:3696489. https://doi.org/10.1155/2020/3696489

Pei Q, Wang X, Zhao L (2020) A sticky rice paste preparation method for reinforcing earthen heritage sites. J Cult Herit 44:98–109. https://doi.org/10.1016/j.culher.2020.01.009

Ren F, Chen W, Zhang J et al (2009) Study on construction techniques of a novel bamboo-steel composite rockbolt. Chin J Rock Mech Eng 28(3):789–793. https://doi.org/10.3321/j.issn:1000-6915.2009.z2.071.(inChinese)

Ren F, Yang Z, Chen J et al (2010) An analytical analysis of the full-range behaviour of grouted rockbolts based on a tri-linear bond-slip model. Constr Build Mater 24(3):361–370. https://doi.org/10.1016/j.conbuildmat.2009.08.021

Ren F, Xu C, Chen W (2012) Numerical simulation on load transfer mechanism of multi-interface composite rockbolt. J Tongji Univ 39(12):1753–1759. https://doi.org/10.3969/j.issn.0253-374x.2011.12.005

Ren F, Zhang F, Xu C et al (2016) Seismic evaluation of reinforced-soil segmental retaining walls. Geotext Geomembr 44(4):604–614. https://doi.org/10.1016/j.geotexmem.2016.04.002

Ren F, Huang Q, Wang G (2020a) Shaking table tests on reinforced soil retaining walls subjected to the combined effects of rainfall and earthquakes. Eng Geol 267:105475. https://doi.org/10.1016/j.enggeo.2020.105475

Ren F, Liu Q, Wang G (2020b) An analytical method for predicting the pullout behavior of embedded planar reinforcements with the consideration of the residual interfacial shear strength. Int J Geosynth Ground Eng 6(3):1–11. https://doi.org/10.1680/gein.2010.17.4.193

Ren F, Li Z, Wang G et al (2018) Centrifugal model tests on anchorage mechanism of rockbolts considering tensile-lateral shearing coupled effect. In: Proceedings of GeoShanghai 2018 international conference (GSIC 2018), Shanghai, China, pp 101–111. https://doi.org/10.1007/978-981-13-0125-4_11

Richards J, Wang Y, Orr SA et al (2018) Finding common ground between United Kingdom based and Chinese approaches to earthen heritage conservation. Sustainability 10(9):3086. https://doi.org/10.3390/su10093086

Richards J, Mayaud J, Zhan H et al (2020) Modelling the risk of deterioration at earthen heritage sites in drylands. Earth Surf Process Landf 45(11):2401–2416. https://doi.org/10.1002/esp.4887

Romanazzi A, Oliveira DV, Silva RA (2019) Experimental investigation on the bond behavior of a compatible TRM-based solution for rammed earth heritage. Int J Archit Herit 13(7):1042–1060. https://doi.org/10.1080/15583058.2019.1619881

Shao M, Li L, Wang S et al (2013) Deterioration mechanisms of building materials of Jiaohe ruins in China. J Cult Herit 14(1):38–44. https://doi.org/10.1016/j.culher.2012.03.006

Spang K, Egger P (1990) Action of fully-grouted bolts in jointed rock and factors of influence. Rock Mech Rock Eng 23(3):201–229. https://doi.org/10.1007/BF01022954

Takase Y (2019) Testing and modeling of dowel action for a post-installed anchor subjected to combined shear force and tensile force. Eng Struct 195(15):551–558. https://doi.org/10.1016/j.engstruct.2019.05.086

Tempa K, Yuden K (2023) Multi-hazard zoning for national scale population risk mapping: a pilot study in Bhutan Himalaya. Geoenviron Disasters 10(1):7. https://doi.org/10.1186/s40677-023-00239-4

Wang D, Cui K, Wu G et al (2022) Comparative study on the anchor performance of wooden tension anchor bolts and tension–compression composite

anchor bolts in earthen sites. Int J Archit Herit. https://doi.org/10.1080/15583058.2022.2031344

Zhang J, Chen W, He F et al (2015) Field tests on anchoring mechanism of the bamboo-steel cable composite anchor with single reinforcement. In: Lollino G, Giordan D, Marunteanu C, Christaras B, Yoshinori I, Margottini C (eds) Engineering geology for society and territory. Springer, Cham, pp 193–197. https://doi.org/10.1007/978-3-319-09408-3_31

Publisher's Note